AD

EDGEWOOD ARSENAL TECHNICAL REPORT

EB-TR-76064

BALLISTIC TEST MATRIX FOR KEVLAR MATERIAL

by

Russell N. Prather
LeRoy W. Metker

Biomedical Laboratory

August 1976

DEPARTMENT OF THE ARMY
Headquarters, Edgewood Arsenal
Aberdeen Proving Ground, Maryland 21010

Disclaimer

The findings in this report are not to be construed as an official position of the US Department of Justice or the Department of the Army unless so designated by other authorized documents.

Disposition

Destroy this report when it is no longer needed. Do not return it to the originator.

UNCLASSIFIED

SECURITY CLASSIFICATION OF THIS PAGE (When Data Entered)

REPORT DOCUMENTATION PAGE	READ INSTRUCTIONS BEFORE COMPLETING FORM
1. REPORT NUMBER: EB-TR-76054	2. GOVT ACCESSION NO. / 3. RECIPIENT'S CATALOG NUMBER
4. TITLE (and Subtitle): BALLISTIC TEST MATRIX FOR KEVLAR MATERIAL	5. TYPE OF REPORT & PERIOD COVERED: Technical Report, Aug [redacted] - Dec [redacted]73
	6. PERFORMING ORG. REPORT NUMBER
7. AUTHOR(s): Russell N. Prather, LeRoy W. Metker	8. CONTRACT OR GRANT NUMBER(s)
9. PERFORMING ORGANIZATION NAME AND ADDRESS: Commander, Edgewood Arsenal, Attn: SAREA-BL-BB, Aberdeen Proving Ground, Maryland 21010	10. PROGRAM ELEMENT, PROJECT, TASK AREA & WORK UNIT NUMBERS: LEAA-[redacted]-005-4
11. CONTROLLING OFFICE NAME AND ADDRESS: Commander, Edgewood Arsenal, Attn: SAREA-TS-R, Aberdeen Proving Ground, Maryland 21010	12. REPORT DATE: Aug [redacted]76; 13. NUMBER OF PAGES: 31
14. MONITORING AGENCY NAME & ADDRESS (if different from Controlling Office): 12 26p.	15. SECURITY CLASS. (of this report): UNCLASSIFIED; 15a. DECLASSIFICATION/DOWNGRADING SCHEDULE: NA

16. DISTRIBUTION STATEMENT (of this Report)

Approved for public release; distribution unlimited.

Copies available from: National Technical Information Service, Springfield, Virginia 22151

17. DISTRIBUTION STATEMENT (of the abstract entered in Block 20, if different from Report)

18. SUPPLEMENTARY NOTES

19. KEY WORDS (Continue on reverse side if necessary and identify by block number)

Soft armor	Discriminant model
Handgun threats	Striking kinetic energy
Backface signature	Blunt trauma
Penetration depth	Gelatin
Penetration volume	

20. ABSTRACT (Continue on reverse side if necessary and identify by block number)

The National Institute for Law Enforcement and Criminal Justice of the Law Enforcement Assistance Administration has established a program to develop an improved lightweight, inconspicuous armor for protection against the more common handgun threats. As a subtask of this program, ballistic tests were conducted for a matrix of materials, plies, and ballistics utilizing behind-the-armor deformation techniques (backface signature). The purpose of these tests was to

(Continued on reverse side)

OVER

DD FORM 1 JAN 73 1473 EDITION OF 1 NOV 65 IS OBSOLETE

UNCLASSIFIED

SECURITY CLASSIFICATION OF THIS PAGE (When Data Entered)

401 007 LB

20. ABSTRACT (Contd)

ascertain in a limited number of experiments any data trends in the backface signature parameters as functions of the incident ballistic parameters and material characteristics.

Except for the small-caliber projectiles, which tend to slip through the weave and defeat the armor, the material backface signature appears to be dependent upon changes in striking kinetic energy, material mass, and material denier.

PREFACE

The work described in this report was authorized and supported by contract LEAA-J-IAA-005-4 awarded by the Law Enforcement Assistance Administration, US Department of Justice, under the Omnibus Crime Control and Safe Streets Act of 1968, as amended. The work was started in August 1973 and completed in December 1973. The experimental data are contained in notebook MN-2549.

Acknowledgments

The authors would like to recognize the assistance given by the following individuals who contributed to this report: Mr. John Holter, who aided in the development of the photographic techniques utilized for the backface signature films; Messrs. Robert E. Carpenter, Lyle C. Snyder, and George J. Maschke, who provided ballistics support; Messrs. James L. Thacker and Ernest Kandel, who provided the electronic support; and Mrs. Myra C. Cohn, who provided extensive data reduction support for the project.

We also wish to acknowledge the supportive efforts of Mr. Nicholas Montanarelli and Mr. Clarence E. Hawkins, Project Officers, and the overall support and administrative guidance received from personnel of the Law Enforcement Assistance Administration, particularly Messrs. Joseph Kochanski, Lester Shubin, and George Schollenberger.

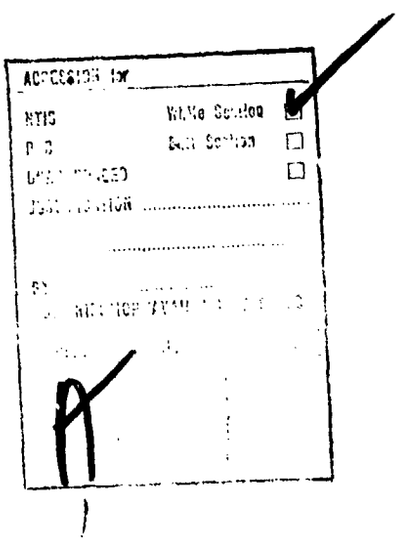

CONTENTS

LIST OF FIGURES

LIST OF TABLES

CONTENTS (Contd)

BALLISTIC TEST MATRIX FOR KEVLAR MATERIAL

I. INTRODUCTION.

The National Institute for Law Enforcement and Criminal Justice (NILECJ) of the Law Enforcement Assistance Administration (LEAA) supports a research and development program to improve and strengthen law enforcement methods. To further this end, studies are being conducted to develop an improved lightweight soft armor for protection against specific street threats; i.e., an armor which will withstand perforation by standard .38-caliber and .22-caliber projectiles and which will also reduce to an acceptable level the blunt trauma associated with the impact of these projectiles upon soft armor.

This report describes the ballistic tests performed within a predefined matrix of materials, plies, and ballistics using techniques developed by personnel of the Biophysics Division to determine "backface signature" or behind-the-armor characteristics.* The more comprehensive matrix which was originally proposed by the Biophysics Division during the initial contract discussions was abbreviated into its present form by personnel of the Aerospace Corporation, the program technical managers. The objective of this abbreviated matrix is to ascertain in a limited number of tests any data trends in th backface sig ature parameters (e.g., volume of deformation, depth of penetration, and deformation time) as functions of the incident ballistic parameters and material characteristics.

II. EXPERIMENTAL METHODS AND PROCEDURES.

A. The Test Matrix.

The test matrix, as defined by LEAA, consisted of the following eight tests:

Test 1: The .38-caliber, 158-grain lead projectile was fired at a nominal velocity of 800 fps against 3, 5, 7, 9, 15, and 23 plies of protective material (Kevlar 29, 400/2 denier, PRD-TL-105-26) to determine the effect of the number of plies on the backface signature.

Test 2. The .38-caliber, 158-grain lead projectile was fired at a nominal velocity of 800 fps against 7 plies of Kevlar 29, 400/2 denier, with material standoffs at 0.5 and 1.0 inch; this was repeated using 15 plies of Kevlar 29, 400/2 denier, at a standoff of 1 inch. The effect of material standoff in conjunction with the number of plies on backface signature was evaluated.

Test 3: To examine the effect of material denier on backface signature, the .38-caliber, 158-grain projectile was launched at a nominal velocity of 800 fps against different deniers of Kevlar material having the same areal density (weight/sq ft) as 7 plies of the Kevlar 29, 400/2 denier, material (approximately 0.44 lb/sq ft). The materials tested were: Kevlar 29, 400/2 denier (PRD-TL-105-26), 400/3 denier (PRD 105-27A), and 1500 denier (PRD 105-628).

*Metker, LeRoy W., Prather, Russell N., and Johnson, Earl M. EB-TR-75029. A Method for Determining Backface Signatures of Soft Body Armors. May 1975.

Test 4: The .38-caliber, 158-grain projectile was fired at nominal velocities of 600, 700, 900, and 1000 fps against 7 plies of Kevlar 29, 400/2 denier, to examine the effect of velocity (varying striking kinetic energy, constant mass) on material performance.

Test 5: The .22-caliber, 40-grain projectile was fired at a nominal velocity of 1000 fps against 7 and 15 plies of Kevlar 29, 400/2 denier. This test, similar to test 1, was designed to examine the effect of the number of plies on the backface signature produced by the .22-caliber missile as well as the effect of a missile of smaller caliber, reduced striking kinetic energy, and higher velocity on the material performance characteristics.

Test 6: The 9-mm, 124-grain jacketed bullet, launched at a nominal velocity of 1150 fps, was fired against 15 and 23 plies of the Kevlar 29, 400/2 denier material in a test similar to tests 1 and 5.

Test 7: Projectiles with diameters of .22 caliber, .32 caliber, and .38 caliber were fired against Kevlar 29 at velocities which yield a striking kinetic energy of 305 joules (225 ft-lb). The missile masses and corresponding test velocities were:

.22-caliber, 40-grain projectile at 1600 fps;

.32-caliber, 101-grain projectile at 1000 fps; and

.38-caliber, 158-grain projectile at 800 fps.

This test was designed to examine the combined effect of missile diameter, mass, and striking velocity on material performance while maintaining a constant striking kinetic energy.

Test 8: Projectiles with a diameter of .38 caliber, launched at velocities of 800, 1000, and 1200 fps, were fired against 7 plies of Kevlar 29. The missile mass was adjusted so that a striking kinetic energy of 305 joules (225-ft-lb) was maintained. The missile masses and corresponding velocities were:

.38-caliber, 70-grain projectile at 1200 fps;

.38-caliber, 101-grain projectile at 1000 fps; and

.38-caliber, 158-grain projectile at 800 fps.

This test was designed to examine the effect of changes in momentum at constant striking kinetic energy.

B. Experimental Method.

Since a detailed explanation of the measurement of the backface signature was reported earlier,* only a cursory explanation will be provided here.

*Metker, LeRoy W., Prather, Russell N., and Johnson, Earl M. EB-TR-75029. A Method for Determining Backface Signatures of Soft Body Armors. May 1975.

High-speed motion picture studies of backlighted gelatin blocks (20% gel) were utilized to record the post-impact deformation of armor into the gelatin.

The equipment used is shown in figure 1 and consists of the following:

1. The weapon, a Mann barrel of the desired caliber, with remote firing capability;

2. A 0.5-meter baseline utilizing a pair of silver grid screens which activate an electronic chronograph (ECI Model 4600) to measure the time of missile flight through the baseline. (The ratio of distance to time yields the velocity at the midpoint of the screens, which is also taken to be the missile striking velocity, drag being considered negligible.)

3. A Redlake Hycam camera focused on the gelatin-armor interface;

4. A large bank of quartz lights to completely backlight the gelatin block;

5. A steel frame which supports the armor material; and

6. The armor material.

During a test the camera was activated and, when the proper framing rate was achieved, a signal was sent to the gun-firing circuit to activate the weapon.

The developed film was "read" on a Model 29E Telereadex film analyzer and the data were processed through the computer program listed in the appendix. This system provided the following data outputs:

1. Precise film speed [pictures per second (pps)];

2. Depth of penetration, X (centimeters);

3. Approximate velocity of deformation [ΔX (centimeters) $\times$ film speed (pps)];

4. Volume of deformation (cubic centimeters);

5. A regression curve which describes the shape of the maximum deformation; and

6. Approximate time of deformation (frames of deformation/pps).

III. RESULTS.

Regression analysis of the data acquired under this program demonstrated that the deformation could adequately be characterized by a paraboloid of revolution. The parabolic equation used to describe the deformation surface in the computer program was of the form

$$y^2 = a + bx$$

where

y = deformation radius

x = deformation depth

a,b = regression constants

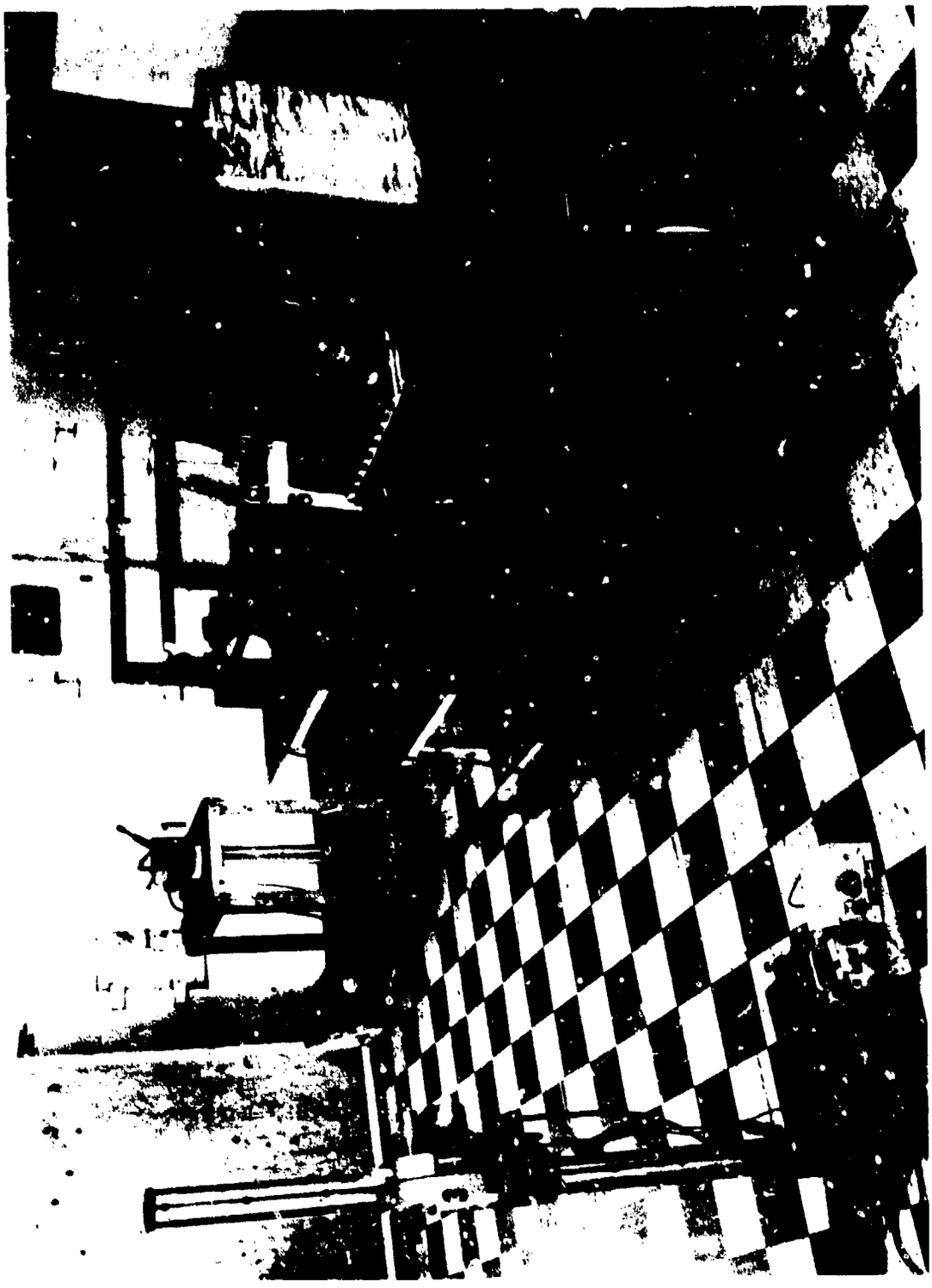

Figure 1. Experimental Setup

The equations defining the deformation surfaces for the tests under this program are listed in tables 1 through 7, along with their corresponding correlation coefficients, root mean square (rms) deviations, maximum deformation depths, and calculated deformation volumes. Plots of some of the test data for which there were sufficient points are shown in figures 2 through 5.

IV. MODELING.

In addition to the backface signature parameters already mentioned, the deformations produced were also characterized by dose levels *similar* to those used in the lethality discriminant models described in the Blunt Trauma Data Correlation study.*

Two provisional models have been proposed under that study. The first, a four-parameter discriminant model, utilizes the maximum number of parameters common to all the published data sets examined. This model, as illustrated in figure 6, accomplishes its discrimination in a plane in which axes X_1, X_2 are defined by

$$X_1 = \ln(MV^2) \text{ and } X_2 = \ln(WD)$$

where

M = projectile mass (grams)

V = projectile impact velocity (meters per second)

W = experimental animal body weight (kilograms)

D = projectile diameter (centimeters)

The discriminant lines establish three zones of low, mid, and high lethality; i.e., as the impact dose increases, the probability of lethality should also increase for targets having the same body weight and for projectiles having the same diameter.

The second model, involving eight parameters, provides better live/die discrimination than the four-parameter model. This model (figure 7) also accomplishes its discrimination in a plane in which axes Y_1, Y_2 are defined by

$$Y_1 = \ln(MV^2/TWD) \text{ and } Y_2 = \ln(L/W)\ (\%APO_2)\ (\%VPO_2)$$

where

M, V, W, D = same as in model 1

T = tissue thickness (centimeters) over the vital organ impacted

L = the total animal lung weight (grams)

$\%APO_2$ = maximum deviation in arterial oxygen pressure from control value

$\%VPO_2$ = maximum deviation in venous oxygen pressure from control value

As in the four-parameter model, the discriminant lines establish zones of nonlethal, mixed, and lethal response for a live/die criterion.

---

*Clare, Victor R., Lewis, James H., Mickiewicz, Alexander P., and Sturdivan, Larry M. EB-TR-75016. Blunt Trauma Data Correlation. May 1975.

Table 1. Test 1 – .38-Caliber, 158-Grain Projectile Versus Kevlar 29, 400/2 Denier

Plies	Striking velocity	Maximum depth	Maximum volume	Deformation time	Surface equation	Correlation coefficient	Root mean square
	fps	cm	cc	sec			
3	812	6.78	203.43	0.0020	$y^2 = 19.42 - 2.9113X$	0.994	0.171
5	805	5.69	182.34	0.0019	$y^2 = 21.82 - 4.0841X$	0.993	0.182
7	800	4.82	155.69	0.0017	$y^2 = 22.21 - 4.9496X$	0.993	0.175
9	794	4.53	166.90	0.0019	$y^2 = 25.81 - 6.2174X$	0.989	0.245
15	813	4.08	176.78	0.0020	$y^2 = 30.46 - 8.1706X$	0.984	0.294
23	815	3.38	113.07	0.0025	$y^2 = 22.73 - 7.1491X$	0.966	0.315

Table 2. Test 2 – .38-Caliber, 158-Grain Projectile Versus Kevlar 29, 400/2 Denier

Plies	Standoff	Striking velocity	Maximum depth	Maximum volume	Deformation time	Surface equation	Correlation coefficient	Root mean square
	in.	fps	cm	cc	sec			
7	0.0*	800	4.82	155.69	0.0017	$y^2 = 22.21 - 4.9496X$	0.993	0.175
	0.5	816	5.70	176.30	0.0020	$y^2 = 22.44 - 4.4190X$	0.973	0.246
	0.5	787	5.48	189.30	0.0023	$y^2 = 25.56 - 5.3145X$	0.969	0.294
	1.0	818	4.78	122.36	0.0020	$y^2 = 19.00 - 4.5404X$	0.958	0.289
15	0.0	813	4.08	176.78	0.0020	$y^2 = 30.46 - 8.1706X$	0.984	0.294
	1.0	821	4.26	159.41	0.0022	$y^2 = 27.48 - 7.3092X$	0.964	0.307

*From test 1.

Table 3. Test 3 – .38-Caliber, 158-Grain Projectile Versus Various Deniers of Kevlar Material

Material	Denier	Striking velocity	Maximum depth	Maximum volume	Deformation time	Surface equation	Correlation coefficient	Root mean square
		fps	cm	cc	sec			
3 Plies - 27A	400/3	815	6.21	144.71	0.0020	$y^2 = 17.08 - 3.1120X$	0.973	0.231
4 Plies - 628	1500	827	CP*	CP*				
7 Plies - 29**	400/2	800	4.82	155.69	0.0017	$y^2 = 22.21 - 4.9496X$	0.993	0.175

*CP - Complete penetration through armor.

**From test 1.

Table 4. Test 4 – .38-Caliber, 158-Grain Projectile Versus 7 Plies of Kevlar 29, 400/2 Denier

Striking velocity	Striking kinetic energy		Maximum depth	Maximum volume	Deformation time	Surface equation	Correlation coefficient	Root mean square
fps	ft-lb	joules	cm	cc	sec			
573	115.63	156.77	4.59	112.68	0.0023	$y^2 = 17.60 - 4.2639X$	0.974	0.194
604	127.83	173.31	4.03	112.25	0.0019	$y^2 = 21.72 - 5.9870X$	0.982	0.231
722	182.74	247.76	4.98	180.08	0.0020	$y^2 = 25.88 - 5.7709X$	0.985	0.224
800*	224.78	304.77	4.82	155.69	0.0017	$y^2 = 22.21 - 4.9496X$	0.993	0.175
904	287.62	389.96	5.53	254.76	0.0020	$y^2 = 32.55 - 6.4687X$	0.988	0.245
1013	360.51	488.30	5.59	221.07	0.0017	$y^2 = 27.91 - 5.4819X$	0.988	0.232

*From test 1.

Table 5. Tests 5 and 6 – Various-Caliber Projectiles, Standard Velocities, Versus Kevlar 29, 400/2 Denier

Projectile		Plies	Striking velocity	Striking kinetic energy		Maximum depth	Maximum volume	Deformation time	Surface equation	Correlation coefficient	Root mean square
caliber	grain		fps	ft-lb	joules	cm	cc	sec			
.22	40	7	1044	96.66	131.05	2.75	56.42	0.0012	$y^2 = 14.25 - 5.6138X$	0.992	0.098
.38	158*	7	800	224.79	304.77	4.82	155.69	0.0017	$y^2 = 22.21 - 4.9496X$	0.993	0.175
.22	40	15	1020	92.45	125.35	2.02	29.02	0.0016	$y^2 = 9.80 - 5.1748X$	0.990	0.114
.38	158*	15	813	232.22	314.85	4.08	176.78	0.0020	$y^2 = 20.46 - 8.1706X$	0.984	0.294
9-mm	124	15	1091	304.74	413.17	CP**	CP**				
.38	158*	23	815	232.22	314.85	3.38	113.07	0.0025	$y^2 = 22.73 - 7.1491X$	0.966	0.315
9-mm	124	23	1059	286.71	388.73	3.66	93.95	0.0017	$y^2 = 16.25 - 4.4149X$	0.954	0.290

*From test 1.

**CP - Complete penetration.

Table 6. Test 7 – Various-Mass Projectiles, 225-ft-lb Striking Kinetic Energy, Versus 16 Plies of Kevlar 29, 400/2 Denier

Projectile		Striking velocity	Striking kinetic energy		Maximum depth	Maximum volume	Deformation time	Surface equation	Correlation coefficient	Root mean square
caliber	grain	fps	ft-lb	joules	cm	cc	sec			
.22	40*	1052	200.51	271.86	3.00	141.05	0.0011	$y^2 = 32.18 - 11.4783X$	0.981	0.227
.22	40*	1545	212.05	287.50	2.66	39.99	0.0008	$y^2 = 9.07 - 3.2210X$	0.950	0.299
.32	101	1056	250.25	339.29	3.15	99.20	0.0011	$y^2 = 20.41 - 6.5935X$	0.995	0.085
.38	158	832	243.59	330.26	4.14	184.03	0.0016	$y^2 = 31.24 - 8.2552X$	0.990	0.243

*Yawed on impact.

Table 7. Test 8 – .38-Caliber Projectile, Varying Mass, 225-ft-lb Striking Kinetic Energy, Versus 7 Plies of Kevlar 29, 400/2 Denier

Projectile		Striking velocity	Striking kinetic energy		Maximum depth	Maximum volume	Deformation time	Surface equation	Correlation coefficient	Root mean square
caliber	grain	fps	ft-lb	joules	cm	cc	sec			
.38	70	1120	194.51	263.72	3.34	91.26	0.0013	$y^2 = 16.30 - 4.5497X$	0.975	0.367
.38	70	1218	230.24	312.16	CP*	CP*				
.38	101	1000	224.52	304.41	4.56	213.88	0.0018	$y^2 = 33.09 - 7.9663X$	0.988	0.221
.38	158**	800	224.79	304.77	4.82	155.69	0.0017	$y^2 = 22.21 - 4.9496X$	0.993	0.175

*CP - Complete penetration.

**From test 1.

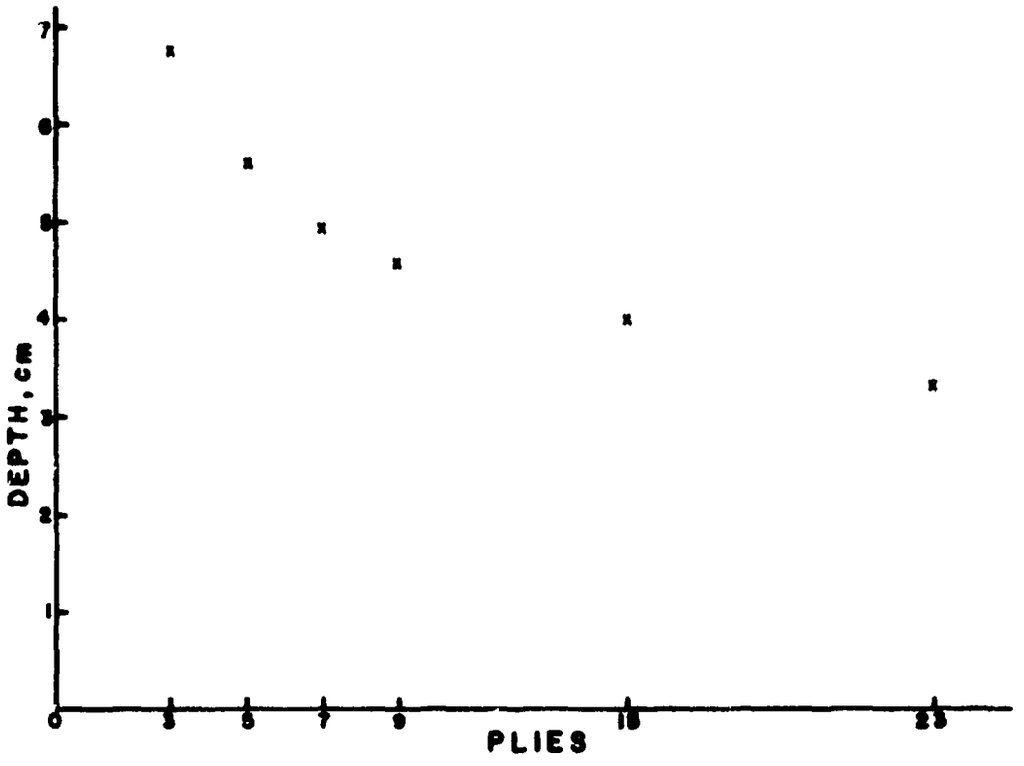

Figure 2. Depth of Penetration into Gelatin for Various Plies of Kevlar 29, 400/2 Denier Material

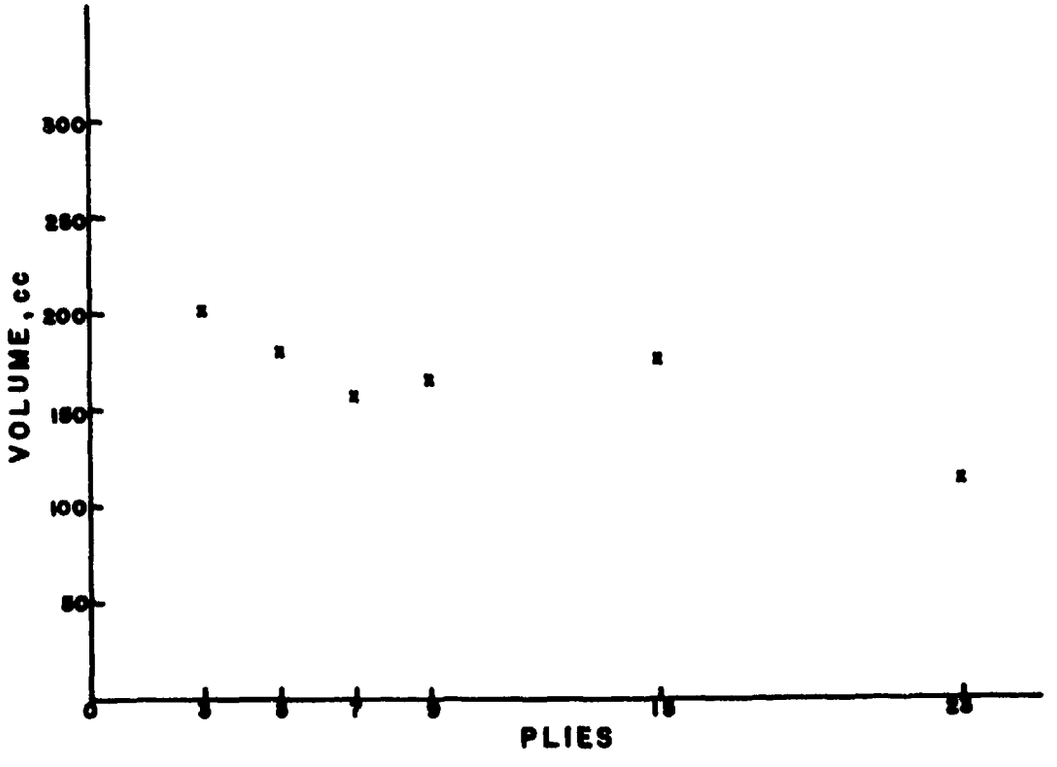

Figure 3. Maximum Deformation Volume in Gelatin for Various Plies of Kevlar 29, 400/2 Denier Material

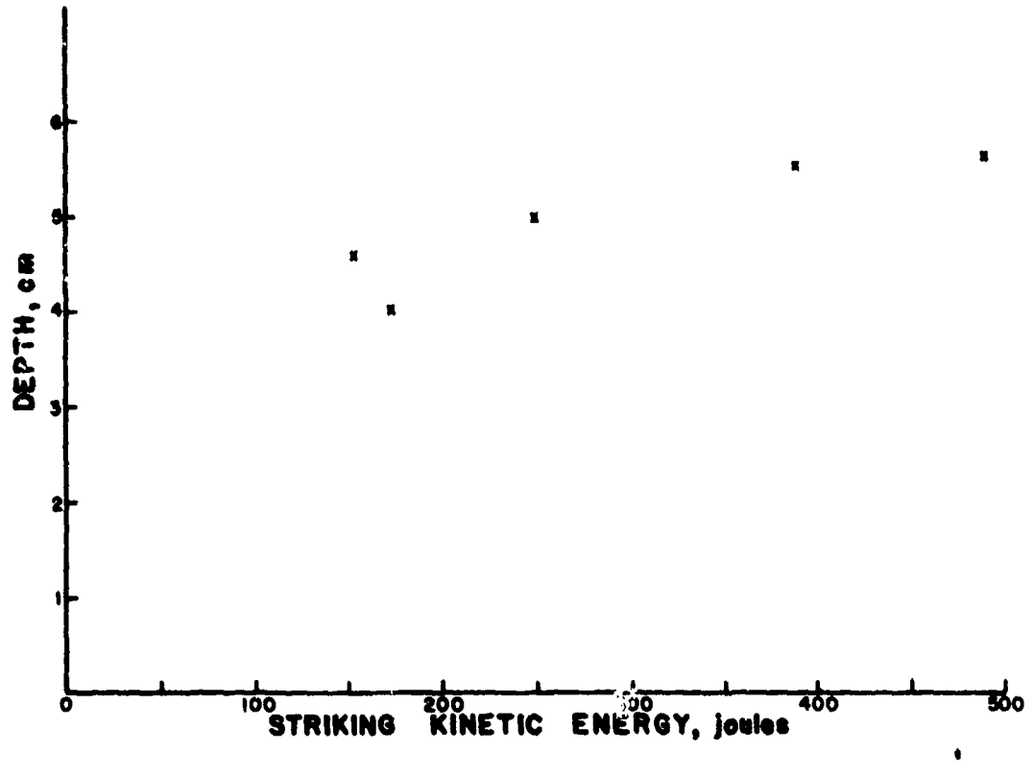

Figure 4. Depth of Penetration of Kevlar 29 into Gelatin for Various Striking Kinetic Energies

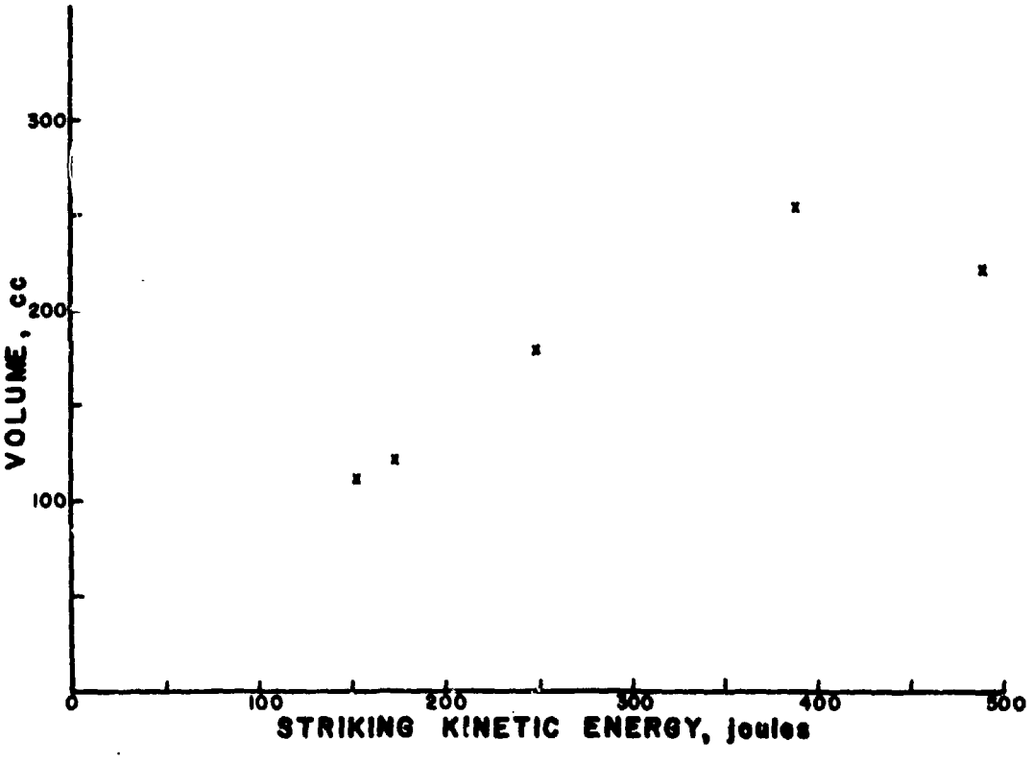

Figure 5. Maximum Deformation Volume of Kevlar 29 in Gelatin for Various Striking Kinetic Energies

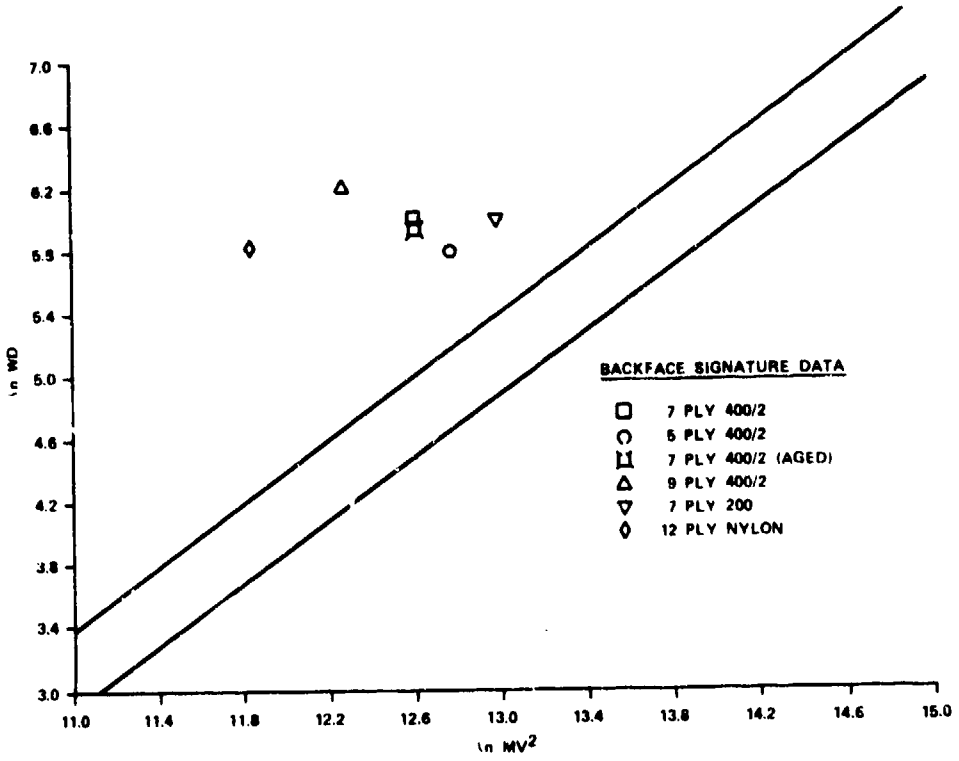

Figure 6. Four-Parameter Lethality Discriminant Model

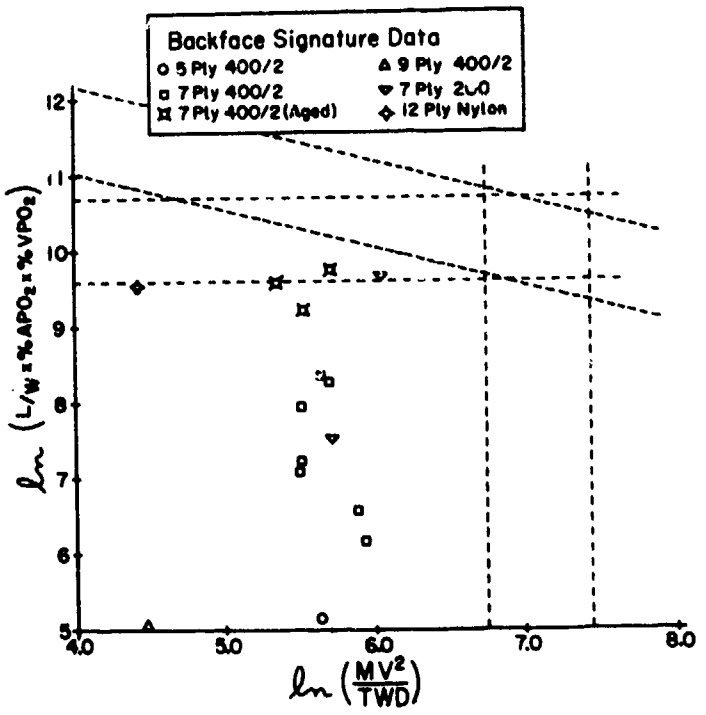

Figure 7. Eight-Parameter Lethality Discriminant Model

These models were formulated from experimental data sets on unarmored animals for which the physical characteristics of the impacting projectile (mass, velocity, diameter) were known. Conditions comparable to those used in the models occur in armor tests when the primary impactor is taken to be that of the missile-material interaction. However, as the armor deforms, the impactor mass and velocity deforming the tissue are changing with time; i.e., the mass is increasing and the velocity is decreasing until at some time "t", depending on the armor deformation characteristics and the tissue response, maximum deformation mass is achieved. At this same point in time, the velocity of the impactor is zero. Thus, a more extensive analysis of the backface signature than that thus far presented is necessary to conform armor deformation to the physical doses used in the models.

1. Velocity.

By employing the principle of the conservation of linear momentum, a pseudo-velocity for the armor deformation was derived:

$$M_p V_p = (M_A + M_p)V$$

or

$$V = M_p V_p/(M_A + M_p)$$

where

M_p, V_p = the initial mass (kilograms) and velocity (meters per second) of the impacting projectile

M_A = the armor deformation mass (kilograms)

V = the "effective" armor velocity (meters per second)

2. Mass.

The mass used in applying the soft armor deformation to the models was that of the projectile-armor mass involved in the maximum deformation. As a conservative approach, the armor mass was assumed to be the mass derived by using the base of the deformation cone; i.e.,

$$M_A = (A_B)\,(a.d.)$$

where

A_B = the base area of the deformation surface (square centimeters)

a.d. = the areal density of the armor material (grams per square centimeter)

These estimates of mass and velocity yield a conservative dose level because the models employ an energy term, MV^2, and the armor mass is used to determine the "effective" velocity behind the armor. If the entire surface mass had been used, a smaller "effective" velocity would then be derived and hence a smaller dose level would be predicted. Furthermore, it is not known at this time whether the deformation of armor involved is due to purely material elongation, slack in sample mounting, or a combination of the two.

Although no animal experiments were involved in the matrix test and none of the physiological response parameters were measured, two approaches were used to illustrate the effects of the physical doses derived from the backface signatures of the various tests. First, the four-parameter model was used and a nominal animal weight of 40 kg was assumed. The dose-response levels for the various test matrix points are listed in table 8. All fall well within the nonlethal zone shown in figure 6.

Secondly, a dose level, $\ln(MV^2/D)$, similar to that used in the eight-parameter lethality model, was derived to provide a relative ranking of the various backface signatures. An analysis of the experimental data used to derive this model revealed that a dose level ≥ 11.0 could produce lethality. Intuitively, it is assumed that, as the dose level decreases, a corresponding decrease in tissue damage will result.

V. CONCLUSIONS.

Test 1. An increase in the number of material plies (increase in material mass) produced an expected decrease in the depth of penetration, volume of deformation, and dose.

Test 2. Standoff produced no significant effect.

Test 3. Kevlar 29, 400/2 denier, was more effective in reducing the depth of penetration than either the 400/3-denier or the 1500-denier material.

Test 4. Increasing the striking velocity of the .38-caliber, 158-grain projectile increased the backface signature.

Tests 5 and 6. These two tests ranked the severity of the more common threats. As one would expect, the backface signature ranked the threats from most severe to least severe as: (1) 9-mm, 124-grain projectile; (2) .38-caliber, 158-grain projectile; and (3) .22-caliber, 40-grain projectile. To defeat the particular 9-mm projectile tested, the use of more than 15 but less than 23 plies of Kevlar 29, 400/2 denier material is required. The .22-caliber projectile, when defeated, produces a significantly lower backface signature than the other two threats.

Test 7. An increase in missile diameter, through the use of standard caliber projectiles, produced little, if any, increase in the backface signature parameters. A constant striking kinetic energy of 305 joules was maintained by adjusting the impact velocities of the .22-caliber (40-grain), .32-caliber (101-grain), and .38-caliber (158-grain) projectiles.

Test 8. Maintaining a constant missile diameter and constant striking kinetic energy by increasing the missile mass and decreasing the velocity appears to have little effect on the backface signature.

Except in the case of small-caliber projectiles, which tend to slip through the weave and defeat the armor, the material backface signature appears to be dependent upon changes in striking kinetic energy, material mass, and material denier. However, the sample size for this test is too small to allow any definite conclusions to be drawn.

Table 8. Dose Levels for Test Matrix Rounds

Test	Projectile		Striking velocity	Material	ln(MV^2)	ln(WD)	ln(MV^2/D)
	caliber	grain	fps				
1	.38	158	812	3-Ply Kevlar 29	12.9	5.9	10.7
			805	5-Ply Kevlar 29	12.7	5.9	10.5
			800	7-Ply Kevlar 29	12.5	5.9	10.3
			794	9-Ply Kevlar 29	12.3	6.0	10.0
			813	15-Ply Kevlar 29	12.0	6.0	9.6
			815	23-Ply Kevlar 29	11.9	5.8	9.8
2	.38	158	800	7-Ply Kevlar 29	12.5	5.9	10.7
			816	7-Ply Kevlar 29, 0.5-inch standoff	12.5	6.0	10.2
			818	7-Ply Kevlar 29, 1.0-inch standoff	12.5	6.0	10.3
			813	15-Ply Kevlar 29	12.0	6.0	9.6
			821	15-Ply Kevlar 29, 1.0-inch standoff	11.8	6.1	9.4
3	.38	158	815	3-Ply 105-27A, 400/3	–	–	–
			827	4-Ply 105-628, 150	CP*	–	–
			800	7-Ply Kevlar 29	12.5	5.9	10.3
4	.38	158	573	7-Ply Kevlar 29	11.9	5.8	9.8
			604	7-Ply Kevlar 29	11.9	5.9	9.7
			722	7-Ply Kevlar 29	12.2	6.1	9.8
			800	7-Ply Kevlar 29	12.5	5.9	10.3
			904	7-Ply Kevlar 29	12.5	6.2	10.0
			1013	7-Ply Kevlar 29	12.8	6.1	10.4
5	.22	40	1044	7-Ply Kevlar 29	11.0	5.8	8.9
			1020	15-Ply Kevlar 29	10.7	5.6	8.7
6	9-mm	124	1091	15-Ply Kevlar 29	CP	–	–
			1059	23-Ply Kevlar 29	12.1	5.7	10.1
7	.22	40**	1502	16-Ply Kevlar 29	10.3	6.1	7.9
	.32	101	1056	16-Ply Kevlar 29	11.7	6.0	9.4
	.38	158	832	16-Ply Kevlar 29	11.8	6.1	9.4
8	.38	71	1120	7-Ply Kevlar 29	12.2	5.7	10.3
	.38	101	1000	7-Ply Kevlar 29	11.8	6.2	9.2
	.38	158	800	7-Ply Kevlar 29	12.5	5.9	10.5

*Complete penetration.

**Missile yawed.

APPENDIX

BACKFACE SIGNATURE COMPUTER PROGRAM

```
      REAL MSE, MSR
      DIMENSION XP(100),YP(100)
      DIMENSION   X(100), Y(100), TITLE(13)
      DIMENSION SM(100)
1000 FORMAT ( 1H1,   19HREGRESSION ANALYSIS
2000 FORMAT  (I2 ,  13A6 )
2500 FORMAT ( 1H   , 13A6  )
3000 FORMAT (2F10.2)
4000 FORMAT (9H     Y =    , F10.4  , 3H+ (  , F10.4 , 3H) X      )
4100 FORMAT (9H     Y =    , F10.4  , 3H+ (  , F10.4 , 8H)LOG(X)   )
4200 FORMAT (9H LOGY =     , F10.4  , 3H+ (  , F10.4 , 8H) X       )
4300 FORMAT (9H LOGY =     , F10.4  , 3H+ (  , F10.4 , 8H)LOG(X)   )
4400 FORMAT (9H 1/Y  =     , F10.4  , 3H+ (  , F10.4 , 8H)LOG(X)   )
4500 FORMAT (9H LOGY =     , F10.4  , 3H+ (  , F10.4 , 8H)1/X      )
4600 FORMAT (9H 1/Y  =     , F10.4  , 3H+ (  , F10.4 , 3H) X       )
4700 FORMAT (9H 1/Y  =     , F10.4  , 3H+ (  , F10.4 , 8H)1/X      )
4800 FORMAT (9H  Y =       , F10.4  , 3H+ (  , F10.4 , 8H)1/X      )
4900 FORMAT (5H Y**    ,F7.4 , 2H = , F10.2 , 3H+ ( , F10.4 , 5H) X**
     1,F7.4   )
5000 FORMAT (1HO, 10X, 14HSTANDARD ERROR   ,12X,  1HT,    //)
5500 FORMAT (2H A  , 2F20.5 ,   5X   15HSIGNIFICANT AT     ,  F6.2 ,
     19H PER CENT      )
5600 FORMAT (2H B  , 2F20.5 ,   5X   15HSIGNIFICANT AT     ,  F6.2 ,
     19H PER CENT      )
5700 FORMAT (1H , 20HANALYSIS OF VARIANCE    , //, 7H SOURCE , 10X,
     12HDF  , 10X , 11HMEAN SQUARE   , 10X  , 1HF  ,// )
6500 FORMAT (11H REGRESSION  , 6X, 1H1 ,  10X ,  F10.5 , 6X , F10.0 ,
     115HSIGNIFICANT AT   ,  F6.2 ,  9H PER CENT  )
6600 FORMAT (6H ERROR    8X , I3 , 10X , F10.5 ,  //, 4H R =      ,
     1F10.5,4X,15HSIGNIFICANT AT  ,  F6.2 ,9H PER CENT ,///)
7000 FORMAT (1H ,12X,3H  X  , 10 X  1HY  , 10X 9HYESTIMATE ,9X,'Y-YEST'
     1//)
8000 FORMAT (1H ,4F15.5)
   1 PY = 1.0
     PX=1.0
     RX-0.0
     WRITE (6,1000)
     READ (5,2000) JTYPE,  (TITLE(I) , I = 1,13)
     WRITE (6,2500)        (TITLE(I) , I = 1,13)
     WRITE (6,21) JTYPE
  21 FORMAT (1H ,I4)
     DO 8 I = 1,100
     READ (5,3000,END = 9 ) XP(I),YP(I)
   8 CONTINUE
   9 N = I - 1
     IF (JTYPE.NE.-1) GO TO 10
```

```
47*          DO 75 JTYPE = 0,8
48*       10 SX = 0.0
49*          SY = 0.0
50*          SXSQ = 0.0
51*          SYSQ = 0.0
52*          SXY = 0.0
53*          M=0
54*          I=0
55*          IF (JTYPE.NE.9)  GO TO 5
56*          READ (5,3000)  PX ,PY
57*       5  CONTINUE
58*          I=I+1
59*          X(I) = XP(I)
60*          Y(I) = YP(I)
61*          IF (JTYPE.EQ.0) GO TO 20
62*          GO TO (11,12,13,14,15,16,17,18,19,19),JTYPE
63*       11 X(I) = ALOG10(X(I))
64*          GO TO 20
65*       12 Y(I) = ALOG10(Y(I))
66*          GO TO 20
67*       13 X(I) = ALOG10(X(I))
68*          Y(I) = ALOG10(Y(I))
69*          GO TO 20
70*       14 X(I) = ALOG10(X(I))
             Y(I)=1.0/Y(I)
72*          GO TO 20
73*       15 X(I) = 1.0/X(I)
74*          Y(I) = ALOG10(Y(I))
75*          GO TO 20
76*       16 Y(I) =  1.0/Y(I)
77*          GO TO 20
78*       17 X(I) = 1.0/X(I)
79*          Y(I) = 1.0/Y(I)
80*          GO TO 20
81*       18 X(I) = 1.0/X(I)
82*          GO TO 20
83*       19 X(I) = X(I)**PX
84*          Y(I) = Y(I)**PY
85*       20 SY = SY + Y(I)
86*          SX = SX + X(I)
87*          SXSQ = SXSQ + X(I)**2.0
88*          SYSQ = SYSQ + Y(I)**2.0
89*          SXY = SXY + X(I)*Y(I)
90*          M=M+1
91*          IF (M.NE.N) GO TO 5
92*       25 CONTINUE
93*          B = (SXY - (SX*SY/FLOAT(N)))/(SXSQ -(SX(SX/FLOAT(N)))
94*          A = (SY/FLOAT(N) - B*SX/FLOAT(N))
95*          MSR = (SXY - SX*SY/FLOAT(N))**2.0/(SXSQ - SX**2.0/FLOAT(N))
96*          DF = FLOAT(N) - 2.0
97*          MSE = ((SYSQ - SY**2.0/FLOAT(N)) -MSR)/DF
98*          F = MSR/MSE
```

```
 99*          CORR =SQRT(MSR/(SXSQ - SY**2.0/FLOAT(N)))
100*          TR = CORR*SQRT(DF/(1.0 - CORR**2.0))
101*          SEA=SQRT(SXSQ*SEB/FLOAT(N))
102*          SEB = SQRT(MSE/(SXSQ - SX**2.0/FLOAT(N)))
103*          TA = A/SEA
104*          TB = B/SEB
105*          IF (JTYPE.EQ.0) GO TO 40
106*          GO TO (41,42,43,44,45,46,47,48,49,49) ,JTYPE
107*       40 WRITE (6,4000) A,B
108*          GO TO 50
109*       41 WRITE (6,4100) A,B
110*          GO TO 50
111*       42 WRITE (6,4200) A,B
112*          GO TO 50
113*       43 WRITE (6,4300) A,B
114*          GO TO 50
115*       44 WRITE (6,4400) A,B
116*          GO TO 50
117*       45 WRITE (6,4500) A,B
118*          GO TO 50
119*       46 WRITE (6,4600) A,B
120*          GO TO 50
121*       47 WRITE (6,4700) A,B
122*          GO TO 50
123*       48 WRITE (6,4800) A,B
124*          GO TO 50
125*       49 WRITE (6,4900) PY,A,B,PX
126*       50 CONTINUE
127*          WRITE (6,5000)
128*          ABTA = ABS(TA)
129*          ABTB = ABS(TB)
130*          IDF = N- 2
131*          VAR1 = STUD(ABTA,IDF)
132*          VAR1 = 100.0*VAR1
133*          VAR2 = STUD(ABTB,IDF)
134*          VAR2 = 100.0*VAR2
135*          WRITE (6,5500)  SEA , TA , VAR1
136*          WRITE (6, 5600)  SEB , TB , VAR2
137*          WRITE ( 6, 5700)
138*          TREG  = SQRT(F)
139*          VAR3 = STUD(TREG,IDF)
140*          VAR3 = 100.0*VAR3
141*          WRITE (6,6500)  MSR , F , VAR3
142*          VAR4 =  STUD(TR,IDF)
143*          VAR4 = 100.0*VAR4
144*          WRITE (6,6600)  IDF , MSE , CORR , VAR4
145*          WRITE (6,7000)
146*          DO 75 I=1,N
147*          YEST=A+B*X(I)
148*          IF (JTYPE.EQ.0) GO TO 60
149*          GO TO (60,62,62,64,62,64,64,60,69,69,69) , JTYPE
150*       62 YEST = 10.0**YEST
```

```
151*          GO TO 60
152*       64 YEST = 1.0/YEST
153*          GO TO 60
154*       69 IF (YEST.LT.0.0) GO TO 80
155*          YEST=YEST**(1.0/PY)
156*       60 SM(I)=YP(I)-YEST
157*          GO TO 81
158*       80 YEST=0.0
159*          SM(I)=0.0
160*          GO TO 93
161*       81 WRITE (6,8000) XP(I),YP(I),YEST,SM(I)
162*          RRX=SM(I)*SM(I)
163*          RX=RX+RRX
164*          GO TO 75
165*       93 WRITE (6,8000) XP(I),YP(I),YEST, SM(I)
166*       75 CONTINUE
167*          RRXX=RX/N
168*          RMS=SQRT(RRXX)
169*          WRITE (6,97) RMS
170*          VOL=3.141592653*XP(1)*A+(3.141592653/2.0)*B*XP(1)**2
171*          PRINT 98,VOL
172*       98 FORMAT (2X,'VOLUME=',F10.5,1X,'CUBIC CENTIMETERS')
173*       97 FORMAT  (///1H ,'RMS = ',F10.5)
174*          GO TO 1
175*          END
```

```
      DIMENSION DIAMY(20),DEPTHX(20),XNEW(20),YNEW(20),CXNEW(20),
     1CYNEW(20),COD(20),COW(20),V(20)
      DIMENSION TITLE(10)
      READ 7,JTYPE,(TITLE(I),I=1,10)
      PRINT 8,(TITLE(I),I=1,10)
      READ 1,M,N,X,Y,PPS
C      M-REPRSEENTS THE NO. OF FRAME COUNTS TO MAX. DEPTH
C      N-REPRSEENTS THE NO. OF DIAMETERS MEASURED FROM MAX DEPTH
      READ 2,(DEPTHX(I),I=1,M)
      READ 2,(DIAMY(I),I=1,N)
      PRINT 9,(DEPTHX(I),DIAMY(I),I=1,N)
    1 FORMAT(5X,I2,5X,I2,5X,F4.0,5X,F4.05X,F5.0)
    2 FORMAT(16F5.0)
      CX=10.0/X
      CY=4.0/Y
      DO 10 I=1,M
   10 COD(I)=DEPTHX(I)*CX
      DO 20 I=1,N
   20 COW(I)=DIAMY(I)*CY
      XINC=DEPTHX(M)/10.0
      XNEW(1)=DEPTHX(M)
      J=0
      DO 30 I=1,10
      K=N-J
      J=J+1
      XNEW(I)=DEPTHX(M)-(FLOAT(I-1)*XINC)
   30 YNEW(I)=DIAMY(K)
      DO 40 I=1,10
      CXNEW(I)=XNEW(I)*CX
   40 CYNEW(I)=YNEW(I)*CY/2.0
      DO 50 I=1,M
   50 V(I)=(COD(I)-COD(I-1))*PPS*10**-2
      TIME=FLOAT(M)*(1.0/PPS)
      PRINT 3,M,N,X,Y,XINC,PPS
      PRINT 4,(CXNEW(I),CYNEW(I),I=1,10)
      PRINT 5,V(1),TIME
      PRINT 5,(V(I),I=2,M)
    3 FORMAT( )
      PRINT 12,(COD(I),COW(I),I=1,N)
   12 FORMAT('0',3X,'DEPTH CONVERSION',10X,'WIDTH CONVERSION',/(3X,
     1F8.4,10X,F8.4))
    4 FORMAT('0',3X,'X',10X,'Y',/(F8.4,3X,F8.4))
    5 FORMAT('0',3X,'VELOCITY',10X,'TIME',/(3X,F8.4,10X,F8.4))
    6 FORMAT(3X,F8.4)
    7 FORMAT(I2,10A6)
    8 FORMAT('1',2X,'FILM NUMBER',2X,10A6)
    9 FORMAT(2X,'RAW VALUES FOR TEST MATRIX',/(2X,F10.5,2X,F10.5))
   11 FORMAT(2F10.2)
      WRITE(7,7) JTYPE,(TITLE(I),I=1,10)
      WRITE(7,11) (CXNEW(I),CYNEW(I),I=1,10)
      CONTINUE
      STOP
      END
```

DISTRIBUTION LIST NO. 2

Names	Copies
EDGEWOOD ARSENAL	
TECHNICAL DIRECTOR	
Attn: SAREA-TD-E	1
FOREIGN INTELLIGENCE OFFICER	1
CHIEF, LEGAL OFFICE	1
CHIEF, SAFETY OFFICE	1
CDR, US ARMY TECHNICAL ESCORT CENTER	1
PUBLIC HEALTH SERVICE LO	8
AUTHOR'S COPY, Biomedical Laboratory	2
DIRECTOR OF BIOMEDICAL LABORATORY	1
Attn: SAREA-BL-M	1
Attn: SAREA-BL-H	1
Attn: SAREA-BL-R	1
Attn: SAREA-BL-RM	1
Attn: SAREA-BL-V	1
DIRECTOR OF CHEMICAL LABORATORY	
Attn: SAREA-CL-B	1
Attn: SAREA-CL-BS	1
Attn: SAREA-CL-BW	1
Attn: SAREA-CL-C	1
Attn: SAREA-CL-D	1
Attn: SAREA-CL-P	1
Attn: SAREA-CL-T	1
Attn: SAREA-CL-T-E	1
DIRECTOR OF DEVELOPMENT & ENGINEERING	
Attn: SAREA-DE-S	1
DIRECTOR OF MANUFACTURING TECHNOLOGY	
Attn: SAREA-MT-E	1
DIRECTOR OF PRODUCT ASSURANCE	
Attn: SAREA-PA-P	1
DIRECTOR OF TECHNICAL SUPPORT	
Attn: SAREA-TS-R	2
Attn: SAREA-TS-L	3
DEPARTMENT OF DEFENSE	
Administrator Defense Documentation Center Attn: Accessions Division Cameron Station Alexandria, VA 22314	12
Director Defense Intelligence Agency Attn: DIR-4G1 Washington, DC 20301	1

Names	Copies
DEPARTMENT OF THE ARMY	
HQDA (DAMO-ODC) WASH DC 20310	1
Director Defense Civil Preparedness Agency Attn: RE(DEP)	1
Attn: PO(DC) Washington, DC 20301	1
Commander-In-Chief US Army Europe & 7A Attn: AEAGC-CNS APO New York 09403	1
Commander US Army-Europe Attn: AEMPS APO New York 09403	1
Chief, Office of Research, Development & Acquisition Attn: DAMA-CSM-CM	1
Attn: DAMA-ARZ-D Washington, DC 20310	1
US Army Research & Standardization Group (Europe) Attn: OCRDA (DAMA-PPI) Box 65, FPO New York 09510	1
OFFICE OF THE SURGEON GENERAL	
HQDA (SGRD-EDE) Attn: LTC Charles Dettor WASH DC 20314	1
Commander US Army Research Institute of Environmental Medicine Attn: SGRD-UE-CA Natick, MA 01760	1
US ARMY HEALTH SERVICE COMMAND	
Commander US Army Environmental Hygiene Agency Attn: USAEHA-AL, Librarian, Bldg 2100 APG-Edgewood Area	1
Commander US Army Institute of Surgical Research Brooke Army Medical Center Fort Sam Houston, TX 78234	1

DISTRIBUTION LIST NO. 2 (Contd)

Names	Copies
US ARMY MATERIEL DEVELOPMENT AND READINESS COMMAND	
Commander US Army Foreign Science & Technology Center Attn: DRXST-IS1 220 Seventh St., NE Charlottesville, VA 22901	2
Commander STIT-EUR APO New York 09710	1
Commander US Army Science & Technology Center-Far East Office APO San Francisco 96328	1
Project Manager for Chemical Demilitarization and Installation Restoration Attn: DRCPM-DR APG-Edgewood Area	1
US ARMY ARMAMENT COMMAND	
Commander US Army Armament Command Attn: DRSAR-ASH Attn: DRSAR-RDT Attn: DRSAR-TDC Rock Island, IL 61201	1 1 1
Commander Dugway Proving Ground Attn: SARDP-TL (Librarian) Dugway, UT 84022	1
Commander Pine Bluff Arsenal Attn: SARPB-ETA Pine Bluff, AR 71611	1
US ARMY TRAININC & DOCTRINE COMMAND	
Commandant US Army Infantry School Combat Support and Maintenance Dept. Attn: NBC Division Fort Benning, GA 31905	1
Commander US Army Armor School Attn: ATSB-CD-MS Fort Knox, KY 40121	1
Commander US Army Infantry School Attn: ATSH-CD-MS-C Fort Benning, GA 31905	1
Commandant US Army Ordnance Center & School Attn: ATSL-CTD-MS-C APG-Aberdeen Area	1
US ARMY TEST & EVALUATION COMMAND	
Record Copy CDR, APG Attn: STEAP-AD-R/RHA APG-Edgewood Area, Bldg E5179	1
CDR, APG Attn: STEAP-TL APG-Aberdeen Area	1
Commander US Army Tropic Test Center Attn: STETC-MO-A (Tech Library) APO New York 09827	1
DEPARTMENT OF THE NAVY	
Chief of Naval Research Attn: Code 443 800 N. Quincy Street Arlington, VA 22209	1
Commander Naval Surface Weapons Center White Oak Laboratory Silver Spring, MD 20910	1
Commander Naval Intelligence Support Center 4301 Suitland Road Washington, DC 20390	1
Commanding Officer Naval Weapons Support Center Attn: Code 5042/Dr. B. E. Douda Crane, IN 47522	1
DEPARTMENT OF THE AIR FORCE	
HQ Foreign Technology Division (AFSC) Attn: PDTR-3 Wright-Patterson AFB, OH 45433	1
HQ, USAF/SGPR Forrestal Bldg WASH DC 20314	1
Commander Aeronautical Systems Division Attn: ASD/AELD Wright-Patterson AFB, OH 45433	1

DISTRIBUTION LIST NO. 2 (Contd)

Names	Copies
Director Air Force Inspection and Safety Center Attn: IGD(AFISC/SEV) Norton AFB, CA 92409	1

Names	Copies
OUTSIDE AGENCIES	
Director of Toxicology National Research Council 2101 Constitution Ave, NW Washington, DC 20418	1
Director Central Intelligence Agency Attn: ORD/DD/S&T Washington, DC 20505	1